

On the Energy Required to Eject Processed Matter from Galaxies

Sergiy Silich^{1,2} and Guillermo Tenorio-Tagle¹

ABSTRACT

We evaluate the minimum energy input rate that starbursts require for expelling their newly processed matter from their host galaxies. Special attention is given to the pressure caused by the environment in which a galaxy is situated, as well as to the intrinsic rotation of the gaseous component. We account for these factors and for a massive dark matter distribution, and develop a self-consistent solution for the interstellar matter gas distribution. Our results are in excellent agreement with the results of Mac Low & Ferrara (1999) for galaxies with a flattened disk-like ISM density distribution and a low intergalactic gas pressure ($P_{IGM}/k \leq 1 \text{ cm}^{-3} \text{ K}$). However, our solution also requires a much larger energy input rate threshold when one takes into consideration both a larger intergalactic pressure and the possible existence of a low-density, non-rotating, extended gaseous halo component.

Subject headings: ISM: bubbles, ISM: abundances, general - starburst galaxies

1. Introduction

The observational evidence of powerful starbursts in dwarf galaxies has led to the idea that, due to their rather shallow gravitational potential, supernova (SN) products and, even the whole of the interstellar medium (ISM), may be easily ejected from the host dwarf systems, causing the contamination of the intra-cluster medium. This issue has been addressed in several papers. De Young & Gallagher (1990) and De Young & Heckman (1994) concluded that typically 1/6 of the shock-wave's swept-up mass may escape its host galaxy, and coherent SN explosions may even totally destroy a galaxy's ISM. More recently, however, Silich & Tenorio-Tagle (1998) and D'Ercole & Brighenti (1999) have shown that within a dark matter (DM) and a low-density extended gaseous halo, a galactic wind does not easily develop, making the removal of the galaxy's ISM very inefficient. Recently, Mac Low and Ferrara (1999, hereafter MF) have used several observational relations to define the galactic dark matter component by means of the central DM density (ρ_c), its maxi-

mum extent (R_h) and its characteristic scale (R_c). They made quantitative conclusions regarding the energetics required for the ejection of metals and of the ISM ("blow-away") from galaxies with an ISM mass in the range ($M_{ISM} = 10^6 - 10^{10} M_\odot$).

In none of the above mentioned studies, however, have the roles of the extragalactic environment nor of the rotation of the interstellar gas been examined in full detail. Meanwhile, Babul & Rees (1992) have indicated that the extragalactic medium pressure (P_{IGM}/k) may vary between 10^{-1} and $10^4 \text{ cm}^{-3} \text{ K}$, making it one of the key parameters in the galactic-extragalactic medium connection.

In the present paper we reexamine the efficiency of starbursts in ejecting their newly produced metals, and in ejecting their whole ISM, from dwarf and normal galaxies, taking into account new boundary and initial conditions. These follow from the pressure equilibrium condition at the galactic-extragalactic boundary, and the relative ability of rotation and interstellar gas pressure to balance different fractions of the galaxy's gravity. In particular, we show that in a self-consistent model, the ISM's gas velocity dispersion and its density at the galaxy center are no longer free parameters, but are defined by the total ISM mass

¹Instituto Nacional de Astrofísica Óptica y Electrónica, AP 51, 72000 Puebla, Mexico

²Main Astronomical Observatory National Academy of Sciences of Ukraine, 03680 Kyiv-127, Golosiiv, Ukraine

(M_{ISM}), the intergalactic pressure (P_{IGM}), and the fraction of the radial component of gravity balanced by pressure gradients. It follows from our considerations that the models of MF which have a low velocity dispersion and a flattened ISM disk-like density distribution, represent a limiting case in the more general scenario of starburst dwarf galaxy evolution.

Section 2 presents the derivation of our model galaxy. Section 3 is devoted to a search for the threshold energy input rate required to expel either metals or the ISM from galaxies with a total ISM mass in the range of 10^6 to $10^9 M_\odot$. Section 4 is a discussion of our results.

2. The Galaxy Model

Our initial model (Silich & Tenorio-Tagle, 1998; hereafter referred to as Paper I) included stars, dark matter, and several isothermal interstellar gas components related to the ionized, neutral and molecular ISM phases. It was in fact an extension to the model developed by Morita (1982), Tomisaka & Ikeuchi (1988), Tomisaka & Bregman (1993) and Suchkov et al. (1994). To be consistent with the approach of MF we have simplified our model by using only the gravitational field imposed by the dark matter (DM) component and using only one of the ISM phases with an effective velocity dispersion C_{ISM} .

The spheroidal DM mass distribution can be approximated by

$$\rho_{DM}(r) = \frac{\rho_c}{1 + (r/R_c)^2}. \quad (1)$$

The DM halo radius (R_h), characteristic scale height (R_c) and central density (ρ_c) are given by MF:

$$R_h = 0.016 \left(\frac{M_{DM}}{M_\odot} \right)^{1/3} H^{-2/3} kpc, \quad (2)$$

$$R_c = 0.89 \times 10^{-5} \left(\frac{M_{DM}}{M_\odot} \right)^{1/2} H^{1/2} kpc, \quad (3)$$

$$\rho_c = 6.3 \times 10^{10} \left(\frac{M_{DM}}{M_\odot} \right)^{-1/3} H^{-1/3} M_\odot kpc^{-3}, \quad (4)$$

where H is the Hubble constant in 100 km s^{-1} units. We adopt $H=0.65$ throughout the paper.

On the other hand, the interstellar gas density and pressure distributions are then defined by (see paper I)

$$\rho_{ISM} = \rho_0 \exp \left[\frac{3}{2} \left(\frac{V_h}{C_{ISM}} \right)^2 \chi \right], \quad (5)$$

$$P_{ISM} = \frac{1}{3} \rho_{ISM} C_{ISM}^2. \quad (6)$$

where ρ_0 is the ISM density at the galactic center, $V_h = \sqrt{\frac{2GM_{DM}}{R_h}}$ is the escape velocity at the DM boundary R_h , G is the gravitational constant and M_{DM} is the DM mass, which is given by

$$M_{DM} = 4\pi \int_0^{R_h} \rho(\omega) \omega^2 d\omega = 4\pi \rho_c R_c^3 [y_h - \arctan(y_h)]. \quad (7)$$

The function χ is

$$\chi = F(\omega) - \epsilon^2 F(r) - (1 - \epsilon^2) F(0), \quad (8)$$

where $r = \sqrt{(x^2 + y^2)}$ and $\omega = \sqrt{(x^2 + y^2 + z^2)}$ are the cylindrical and spherical radii, respectively, and the dimensionless radii $y_\omega = \omega/R_c$ and $y_h = R_h/R_c$. The factor $(1 - \epsilon^2)$ is the fraction of the radial component of gravity that is balanced by pressure gradients (Tomisaka & Ikeuchi, 1988). The case $\epsilon = 1$ implies a full balance between the radial component of gravity and the circular rotation of the galaxy, whereas $\epsilon = 0$ implies spherically symmetric systems without rotation. The function F was defined in paper I and, in the case of a potential exerted by DM only, it becomes:

$$F(\omega) = 1 + \frac{R_h}{R_c} \frac{4\pi \rho_c R_c^3}{M_{DM}} \times \left[\frac{1}{2} (\ln(1 + y_h^2) - \ln(1 + y_\omega^2)) + \frac{\arctan(y_h)}{y_h} - \frac{\arctan(y_\omega)}{y_\omega} \right],$$

for $\omega \leq R_h$, (9)

$$F(\omega) = \frac{R_h}{\omega}, \quad \text{for } \omega > R_h, \quad (10)$$

The DM mass is related to the visible mass by (MF)

$$M_{DM} = 3.47 \times 10^8 \left(\frac{M_{ISM}}{10^7 M_\odot} \right)^{0.71} M_\odot. \quad (11)$$

One can also include a transition from a rotating disk to a non-rotating spherical halo by expressing the ϵ in equation (8) as

$$\epsilon = \epsilon_c / \exp[(z/H_z)^2 + (r/H_r)^2], \quad (12)$$

where ϵ_c is the value of ϵ at galactic center. This prevents the funnel-like density distribution that develops around the symmetry axis (see Suchkov et al. 1994). However, to be consistent with the considerations of MF, we have set the scale-lengths H_z and H_r to be much greater than or comparable to the DM halo radius.

Following MF we assume that the interstellar gas extends out to a cutoff radius R_{ISM} given by

$$R_{ISM} = 3 \left(\frac{M_{ISM}}{10^7 M_\odot} \right)^{0.338} \text{ kpc}. \quad (13)$$

However, we further assume that the galaxy is stable and that the ISM is in pressure balance with the intercluster gas at the galaxy outer boundary ($P_{ISM} = P_{IGM}$). This defines the ISM gas density at the galaxy outer edge to be

$$\rho_G = \frac{3P_{IGM}}{C_{ISM}^2}. \quad (14)$$

Thus, given the total mass of the ISM (M_{ISM}) and the pressure of the intergalactic medium (P_{IGM}), only ρ_0 and C_{ISM} must be found for fully defining the ISM mass distribution. This can be achieved by solving a system of two nonlinear equations

$$4\pi \int_0^{R_h} \int_0^{R_h} \rho_{ISM}(r, z) r dr dz = M_{ISM} \quad (15)$$

$$P_{ISM}(R_{ISM}, 0) = P_{IGM}, \quad (16)$$

where $\rho_{ISM}(r, z)$ and $P_{ISM}(r, z)$ are defined by the equations (5) and (6). Note that $\rho_{ISM}(r, z)$ should be set equal to zero whenever its calculated value falls below ρ_G . The equations can be solved by an iterative method of high accuracy. Thus, in a self-consistent model, the ISM gas velocity dispersion and gas density at the galaxy's center are no longer free parameters, but are determined by the total ISM mass M_{ISM} , the extragalactic pressure P_{IGM} , and the fraction of the radial component of gravity balanced by pressure gradients.

Figure 1 presents as an example, the ISM density distribution for $M_{ISM} = 10^8 M_\odot$ models with

different fractions (ϵ^2) of the radial component of gravity balanced by the centrifugal forces. The figure shows the smooth transition from a flattened disk-like system dominated by fast rotation (Panel a) to a spherical, non-rotating galaxy (Panel c).

3. Energy requirements

Once a nuclear coeval starburst has all its stars on the main sequence, it begins to build a superbubble. In a constant density medium, the shock enters a phase of continuous deceleration from the very beginning of the superbubble evolution. However, if the starburst is placed in a plane with a stratified decreasing gas density, it will expand furthest in the direction of least resistance, deforming the originally round superbubble into an elongated remnant along the symmetry axis. In the case of an exponentially-decreasing density distribution, the remnant will then break out if the leading shock reaches a couple of galactic scale heights (H_e) while maintaining a supersonic speed, V_S (Kompaneets 1960, Koo & McKee 1992), while in a Gaussian atmosphere the shock acceleration starts once it reaches a galactic scale-height H_g (Koo & McKee 1990). As $V_S = (P_{bubble}/\rho_Z)^{0.5}$, where P_{bubble} is the interior pressure, and ρ_Z is the ISM density that decreases sharply along the Z axis, the shock is forced to accelerate. Once in the acceleration phase, neither the external gas pressure nor the galaxy's gravitational potential can restrain the shock, which ultimately will acquire speeds larger than the galactic escape velocity (V_{esc}). This occurs even if $V_s < V_{esc}$ prior to the acceleration phase that begins at $Z \sim$ the gaseous scale-height. It is also well known that the swept up matter immediately behind the accelerating shock, also accelerates, producing the onset of Rayleigh-Taylor instabilities that fragment the swept-up matter shell. The remnant is then able to "blowout", driving its high pressure gas between the fragments into the halo of the host galaxy, where it once again will push the shock (see Tenorio-Tagle & Bodenheimer 1988, and references therein).

The minimum starburst energy input rate (L_{cr}), that leads to breakout, continuous acceleration, and expulsion of matter from galaxies into the IGM, either from a Gaussian or an exponential atmosphere was studied by Koo & McKee

(1992). The authors used the threshold luminosity criterion ($L_{breakout}$) which assures that the shock will reach one scale height H while maintaining a supersonic speed:

$$L_{breakout} = 17.9\rho_0 H^2 C_{ISM}^3 \text{ ergs s}^{-1} \quad (17)$$

For an exponential atmosphere, Koo & McKee (1992) demand an $L_{cr} \geq 3L_{breakout}$. In a Gaussian density distribution the acceleration phase starts earlier, and thus we shall assume $L_{cr} \geq L_{breakout}$. Note, that in the flattened disk-like configurations, the characteristic scale height H may exceed the thickness of the galaxy's disk Z_{ISM} , requiring that H in the equation (17) be replaced by Z_{ISM} .

3.1. The Density Distribution along the Axis of Symmetry

Applying the breakout criterion to our model galaxies required accurate fits to the resultant density distributions (see Section 2) along the symmetry axis.

3.1.1. Disk-like density distributions

In the case of flattened disk-like distributions, one can show that near the galaxy's plane the resultant gas density distribution along the symmetry axis is fitted well by a Gaussian function:

$$\rho_{ISM} = \rho_0 \exp[-(Z/H_g)^2], \quad (18)$$

with the characteristic scale height

$$H_g = \sqrt{\frac{C_{ISM}^2}{2\pi G \rho_c}}. \quad (19)$$

Further away from the galaxy's plane, the density distribution can be well approximated by an exponential function

$$\rho_{ISM} = \rho_G \exp[(Z_{ISM} - Z)/H_e], \quad (20)$$

where Z_{ISM} is the disk thickness along the Z axis. As the match to the density distribution requires two different functions, we have restricted the parameter H_e by the condition that the density gradient, as given by the functions (18) and (20), must be smooth and continuous at the crossing point (Z_f). This condition can be represented by

the following two equations:

$$\log \rho_0 - \left(\frac{Z_f}{H_g}\right)^2 \log(e) = \log \rho_G + \frac{Z_{ISM} - Z_f}{H_e} \log(e), \quad (21)$$

$$\frac{2Z_f}{H_g^2} \log(e) = \frac{1}{H_e} \log(e). \quad (22)$$

Solving for H_e and Z_f gives:

$$H_e = \frac{1}{2} \frac{Z_{ISM}^2}{Z_f}, \quad (23)$$

$$Z_f = Z_{ISM} \times \left[1 - \sqrt{1 - \left(\frac{H_g}{Z_{ISM}}\right)^2 \frac{\log(\rho_0/\rho_G)}{\log(e)}} \right], \quad (24)$$

which uniquely define the intersection point Z_f and the fitting parameter H_e required in estimating the minimum energy input rate for breakout.

The ISM distribution along the Z axis for different disk-like galaxies and different extragalactic gas pressures (solid lines) and their analytic fit (dashed lines) are shown in the Figures 2 a and b.

3.1.2. Spherical density distributions

The ISM density distribution for different galaxies under the assumption of $\epsilon = 0$, and different extragalactic gas pressures are shown in Figures 2 c and d. In these cases the density distribution far from the galaxy's plane cannot be fitted by a Gaussian or an exponential function. Thus to estimate the minimum energy input rate required to eject the metals from these galaxies we have only used the numerical scheme of paper I. In all cases we have assumed a constant mechanical energy input rate during the starburst supernova phase (4×10^7 yr).

3.1.3. The energy requirements

Our galaxy models are summarized in Table 1. The various models are labeled with several indexes that represent the logarithm of the ISM mass considered, ϵ values that range between 0 and 0.9, and intergalactic gas pressure (P_{IGM}/k) values that are assumed to be either 1 or 100 cm^{-3}

K. In the Table, column 1 gives the model identification. Columns 2 and 3 list the DM and ISM masses, column 4 gives the ISM cutoff radius, column 5 the intra-cluster gas pressure (P_{IGM}), and columns 6 and 7 show the interstellar gas velocity dispersion and escape velocity at the galaxy boundary R_{ISM} . The central gas number density is shown in column 8 and column 9 shows the ISM extent along Z axis (Z_{ISM}).

Figure 3 shows our energy estimates resultant from the numerical integration of the hydrodynamic equations for a coeval starburst with a constant energy input rate during the first 4×10^7 yr of the evolution, and the initial density distributions shown in Figure 2 a - d. Figure 3 considers a range of galactic ISMs (from 10^6 to $10^9 M_\odot$) and extreme values of ϵ ($= 0.9$ for flattened disk-like density distributions and $= 0$ for spherical galaxies without rotation) and also for a range of values of P_{IGM}/k (equal to 1 and $100 \text{ cm}^{-3} \text{ K}$). Our results for disk-like gas distributions are in excellent agreement with the findings of MF, particularly for the case of $P_{IGM}/k = 1 \text{ cm}^{-3} \text{ K}$. Note, however, that the threshold energy input rate in our models depends on the intergalactic gas pressure, P_{IGM} , and becomes rapidly larger for smaller M_{ISM} and larger P_{IGM} .

In the case of the flattened disk-like configurations ($\epsilon = 0.9$; see Table 1), our numerical experiments indicate that the shock acceleration phase starts after $1.2 - 1.4 H_g$, and thus it is the Gaussian rather than the exponential outer part of the disk-like density distributions the ones that define the onset of shock acceleration. Our results are in good agreement with the analytic criterion that ensures breakout (equation (17)) from the density distributions shown in Figure 2 a and b, particularly when the values of the Gaussian scale-height ($H = H_g$) are used (filled symbols in Figure 3).

In Figure 3, values below each line imply total retention, while the region above each line indicates the expulsion of the hot superbubble interior gas (the new metals) out of disk-like distributions ($\epsilon = 0.9$), and of the new metals and the whole of the ISM in the spherical ($\epsilon = 0$) cases. Each line that separates the two regions marks the minimum energy input rate needed from a coeval starburst to reach the outer boundary of a given galaxy, regardless of the time that the remnant may require to do so. In the case of disk-

like configurations, this energy input rate warrants breakout and the ensuing continuous acceleration. In most of these cases the ejection of the hot gas into the intergalactic medium occurs before the starburst supernova phase is over ($4 \times 10^7 \text{ yr}$). In galaxies with $\epsilon = 0$, however, the evolution time considered largely exceeds the starburst supernova phase. This causes the decelerating shell of interstellar swept up matter to reach the galaxy edge by means of the momentum gathered during its early evolution. Figure 4 shows the results for a $M_{ISM} = 10^8 M_\odot$ galaxy under two extremes of intergalactic pressures ($P_{IGM}/k = 1$ and $100 \text{ cm}^{-3} \text{ K}$) as they become expelled by the lower limit mechanical energy input rate displayed in Figure 3. Throughout its evolution, the remnant in the high pressure galaxy undergoes a continuous deceleration, while the low pressure system is able to experience the acceleration promoted by breakout. In both cases however, the time needed to reach the galaxy outer boundary is much larger than the supernova phase and thus both remnants slow down by conservation of their own momentum, to reach the galaxy boundary and experience total disruption after 100 Myr and 200 Myr of evolution in the high and low intergalactic pressure cases, respectively.

The right-hand axis in our summary Figure 3 indicates the mass of the coeval starburst able to produce the energy input rate indicated in the left-hand axis. This has been scaled from the synthesis models of Leitherer & Heckman (1995) for a $10^6 M_\odot$ starburst under the assumption of a Salpeter IMF with a lower mass limit of $1 M_\odot$, an upper stellar mass equal to $100 M_\odot$, and a metallicity $Z = 0.1$. In this case, the log of the mechanical energy input rate in erg s^{-1} is 40.5, and scales linearly with the starburst total mass.

In Figure 3, we have also indicated the results of another two calculations where we assumed a gravitational potential corresponding to a $M_{ISM} = 10^9 M_\odot$ galaxy. In these two models however, we have adopted a spherical halo with total masses of $10^8 M_\odot$ and $10^7 M_\odot$ and an intergalactic gas pressure equal to $P_{IGM}/k = 1 \text{ cm}^{-3} \text{ K}$. The derived minimum energy input rate (or minimum mass of the coeval starburst required to expel the ISM) clearly indicates that it is the mass of the halo, instead of the disk component, what determines the minimum energy input rate necessary for ejec-

tion. Figure 3 shows that a halo with only 1/100 of the mass of the disk-like configuration ($M_{ISM} = 10^9 M_{\odot}$) increases the value of the minimum energy input rate required for mass ejection by approximately an order of magnitude. An energy input rate nearly two orders of magnitude higher is needed if the spherical halo has a mass of 1/10 of the disk-like configuration.

4. Discussion

We have described a simple, self-consistent, approach to build the ISM gas distribution of galaxies, accounting for the gravitational potential exerted by a massive DM component, as well as for rotation of the ISM and the intergalactic gas pressure. The numerical experiments and analytical estimates have then showed that the final fate of the matter ejected from a starburst region, as well as that of the shocked ISM, is highly dependent on the boundary conditions. Following a continuous transition from a fast rotating, thin, disk-like to a spherical non-rotating interstellar gas distribution, we have found that the ISM to be more resistant to ejection than estimated in earlier papers.

We have shown (see Figure 3) that superbubbles evolving in galaxies that have a gaseous disk-like density distribution are likely to undergo the phenomenon of breakout. This allows them to accelerate and expel all of their newly produced metals, and perhaps even a small fraction of the interstellar medium, into intergalactic space. On the other hand, much larger energy input rates, or more massive coeval starbursts (up to 3 orders of magnitude larger), are required to provoke breakout or push a shell to the galaxy outer boundary for a spherically-symmetric ISM mass distribution. Even low mass ($\sim 1\%$ - 10% of the total ISM mass), non-rotating subsystems increase the energy requirements by more than an order of magnitude. This makes the low density haloes, rather than DM itself, the key component in the evolution of dwarf galaxies.

The halo properties, on the other hand, are highly dependent on the gravitational potential. The presence of an extended DM component makes the halo mass distribution more smooth and extended. However, the halo parameters are also dependent on the properties of the intergalactic medium. To withstand a high intergalactic pres-

sure, the halo has to support itself with a high random motion, which leads to a more homogeneous gas distribution compared to that found in low pressure surroundings.

Clearly the energy input rates derived here are lower limits to the amounts required for expelling matter from a galaxy. Particularly because only one component of the ISM was considered and because the central densities adopted are well below the values expected for the star forming cloud where the starburst originated. Our estimates thus neglect the effect of the starburst plowing into the parental cloud material. These are lower limits also because we adopted a constant energy input rate (see Strickland & Stevens 2000) and because our approach neglects an additional cooling by mass-loading process (Hartquist et al. 1986) and the presence of a magnetic field which also could inhibit expansion (Tomisaka 1998).

The indisputable presence of metals (in whatever abundance) in galaxies implies that the supernova products cannot be lost in all cases. Note in particular that many well known disk galaxies have a high metal abundance and a large number of centers of star formation. Most of these exciting star clusters are more massive than the $10^4 M_{\odot}$ lower limit established by MF and the current paper as the minimum starburst mass required to cause mass ejection in the case of disk-like systems. This lower limit for disk-like galaxies with $M_{ISM} \leq 10^9 M_{\odot}$ (see Figure 3) implies that starbursts even smaller than the Orion cluster would break through the galaxy outer boundary and eject their supernova products into the intergalactic medium. Nevertheless, disk-like galaxies can avoid losing all their freshly produced metals by having a halo component, neglected in former studies, that acts as the barrier to the loss of the new metals.

The haloes, despite acting as the barrier to the loss of the new metal, have rather low densities ($\langle n \rangle \sim 10^{-3} \text{ cm}^{-3}$) and thus have a long recombination time ($t_{rec} = 1/(\alpha n_{halo})$; where α is the recombination coefficient) that can easily exceed the life time of the HII region ($t_{HII} = 10^7 \text{ yr}$) produced by the starburst. In such a case, the haloes may remain undetected at radio and optical frequencies (see Tenorio-Tagle et al. 1999), until large volumes are collected into the expanding supershells. Note that the continuous Ω shape

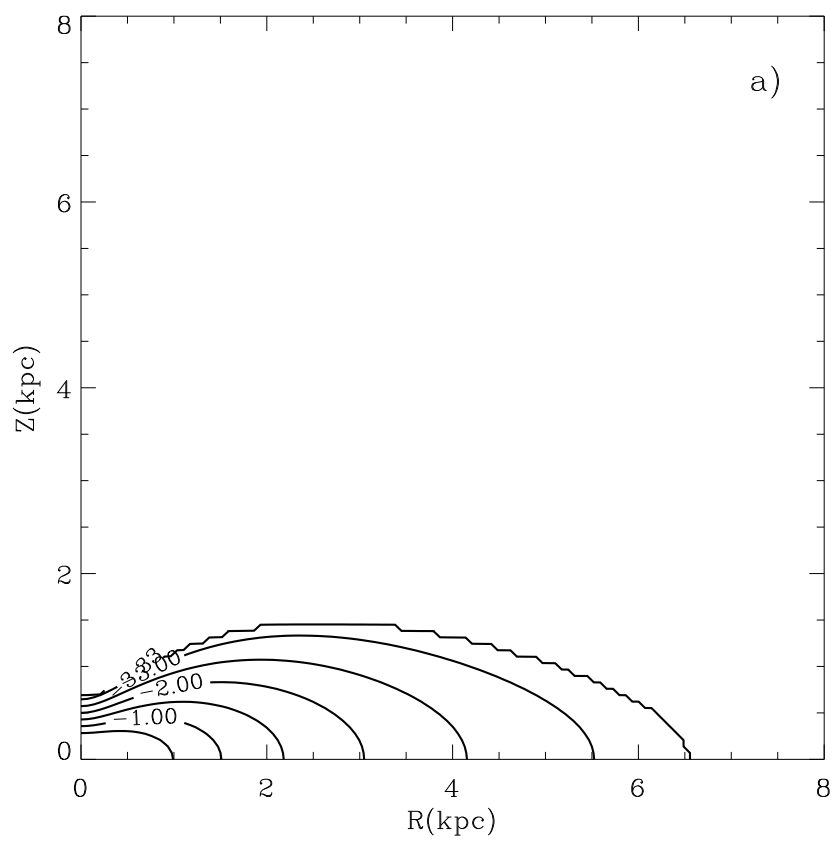
that supershells present in a number of galaxies, while remaining attached to the central starburst, and their small expansion velocity (comparable or smaller than the escape velocity of their host galaxy) imply that the mechanical energy of the star cluster is plowing into a continuous as yet undetected medium. Other authors (see MF 1999) have argued that blowout could leave fragments of the dense shell behind and that these observed with poor resolution may appear to form a continuous shell much smaller than the true extent of the shocked region. Clearly, X-ray observations of these supershells will help to decide if the hot processed material is enclosed or not by the expanding shell.

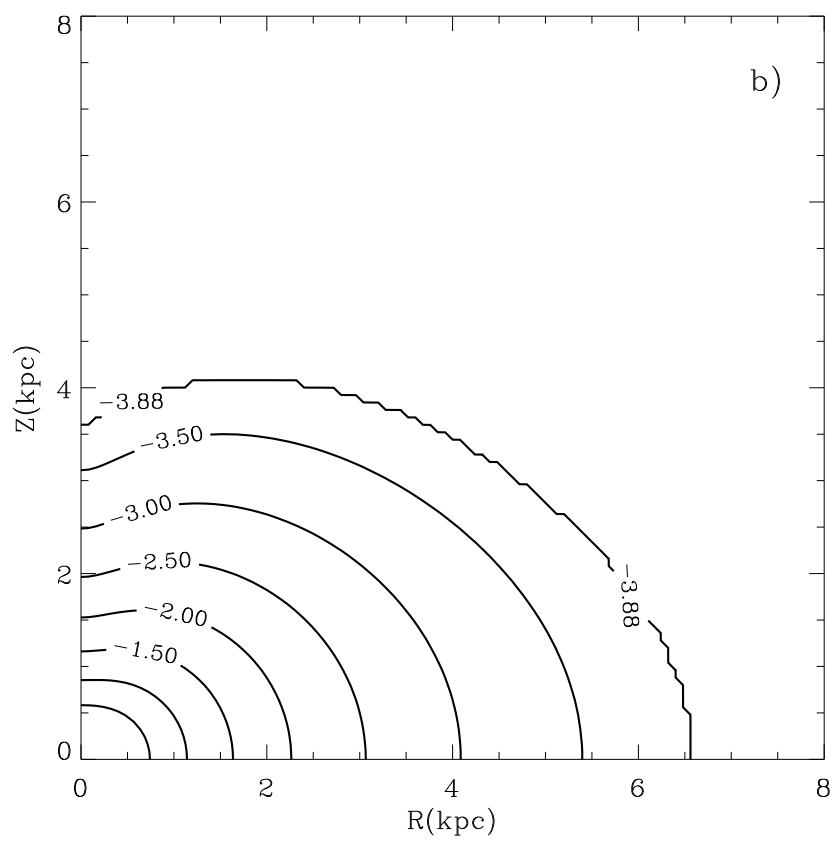
Thus the answer, the true limit for mass ejection from galaxies, must lie between the two extreme cases that we have investigated here. Note however, that in the presence of a halo, it is the mass of the halo that sets the limiting energy input rate required for mass ejection, and not the mass of the disk-like component. This argument applies to all galaxies whether spirals, amorphous irregulars or dwarfs.

We are grateful to our referee Dr. M-M. Mac Low for a speedy processing of our paper and the various comments that help to improve it. We also thank W. Wall for his careful reading of our manuscript. GTT also thanks CONACYT for the grant 211290-5-28501E which allowed for the completing of this study.

REFERENCES

- Babul, A. & Rees, M. 1992, *Mon. Not. Roy. Ast. Soc.*, 255, 346
- D’Ercole, A. & Brighenti, F. 1999, *Mon. Not. Roy. Ast. Soc.*, 309, 941
- De Young, D. & Gallagher, J. 1990, *ApJL*, 356, L15
- De Young, D. & Heckman, T. 1994, *ApJ*, 431, 598
- Hartquist T.W., Dyson J.E., Pettini M. & Smith L.J. 1986, *Mon. Not. Roy. Ast. Soc.*, 221, 715
- Kompaneets, A.S. 1960, *Soviet Phys. Doklady*, 5, 46
- Koo, B-C., McKee, C.F. 1990, *ApJ*, 354, 513
- Koo, B-C., McKee, C.F. 1992, *ApJ*, 388, 93
- Leitherer, C. & Heckman, T.M. 1995, *ApJS*, 96, 9
- Mac Low, M-M. & Ferrara, A. 1999, *ApJ*, 513, 142 (MF)
- Morita, K. 1982, *PASJ*, 34, 65
- Silich, S. & Tenorio-Tagle, G. 1998, *Mon. Not. Roy. Ast. Soc.*, 299, 249 (Paper I)
- Strickland D.K. & Stevens I.R. 2000, *Mon. Not. Roy. Ast. Soc.*, 314, 511
- Suchkov, A., Balsara, D., Heckman, T. & Leitherer, C. 1994, *ApJ*, 430, 511
- Tenorio-Tagle, G. & Bodenheimer, P. 1988, *ARA&A*, 26,145
- Tenorio-Tagle, G, Silich, S., Kunth, D., Terlevich, E. & Terlevich, R. 1999, *Mon. Not. Roy. Ast. Soc.*, 309, 332
- Tomisaka, K. & Ikeuchi, S. 1988, *ApJ*, 330, 695
- Tomisaka, K. & Bregman, J.N. 1993, *PASJ*, 45, 513
- Tomisaka, K. 1998, *Mon. Not. Roy. Ast. Soc.*, 298, 797





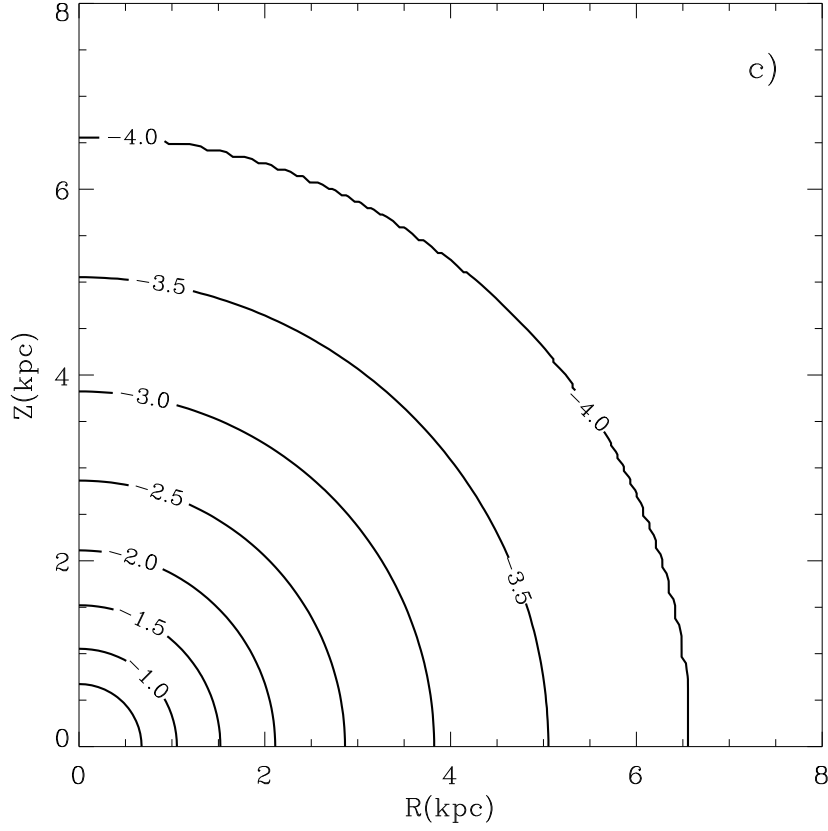
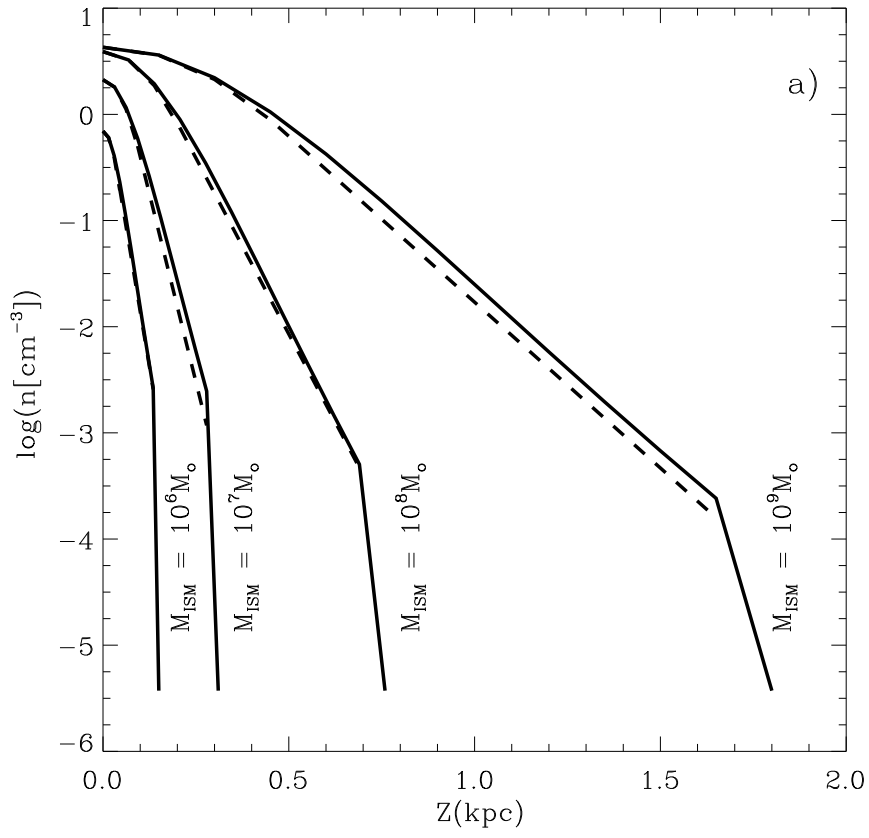
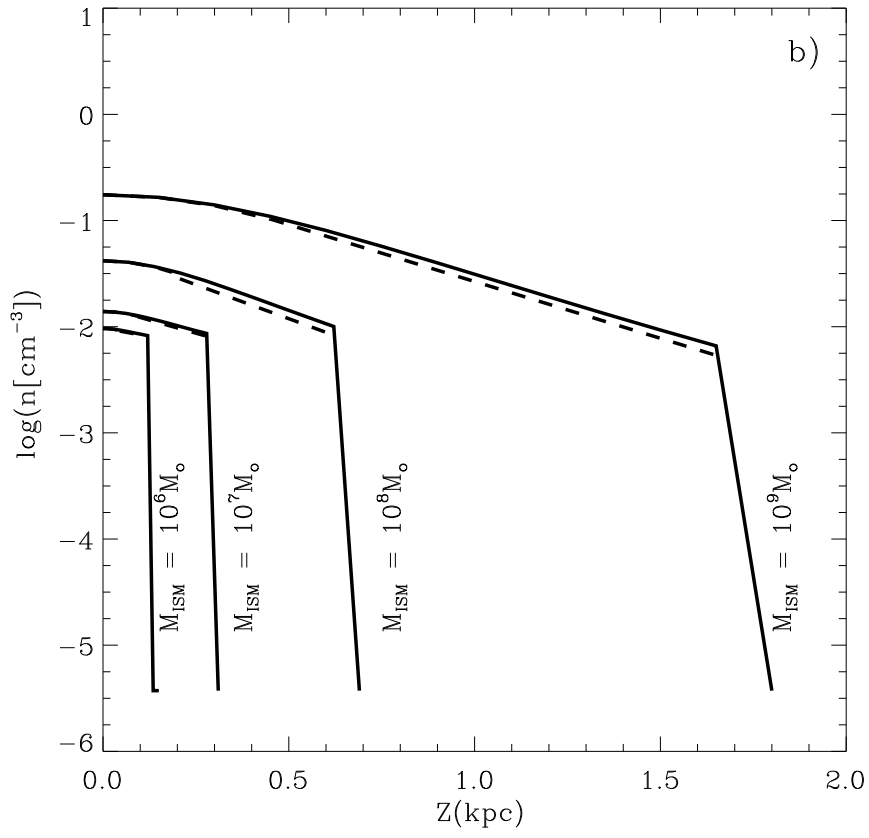
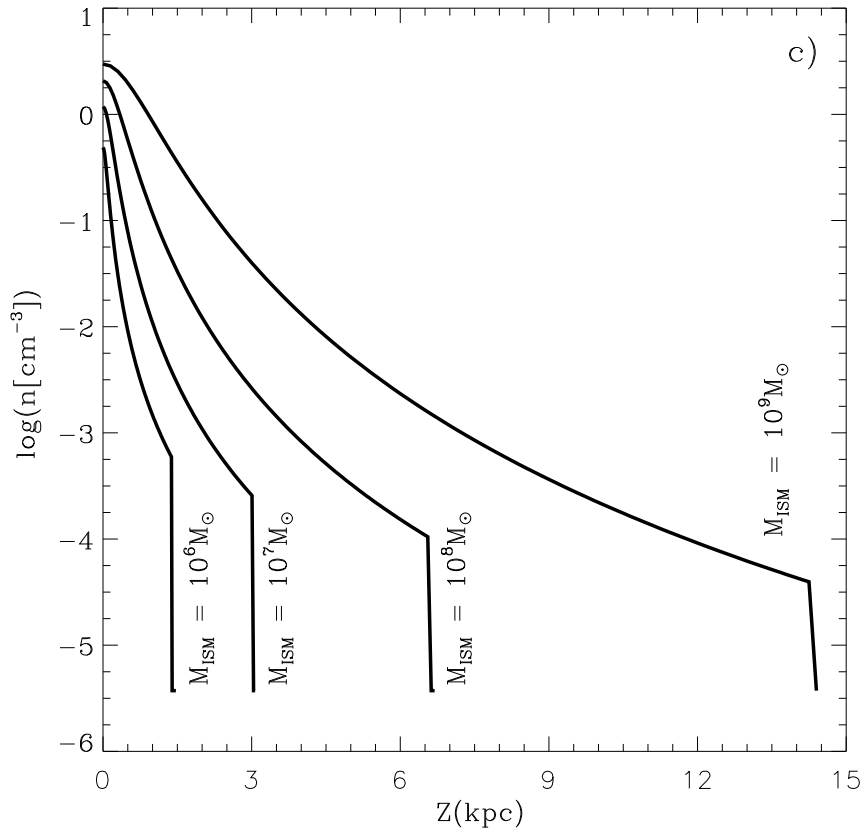


Fig. 1.— The model galaxy. Logarithmic contours showing the density distribution for a galaxy with a $M_{ISM} = 10^8 M_{\odot}$ and a $P_{IGM}/k = 1 \text{ cm}^{-3} \text{ K}$ and several values of ϵ ($= 0.9, 0.5$, and 0.0). The latter correspond to the fraction $f = 1 - \epsilon^2$ equal to 19%, 75% and 100% of the radial component of gravity balanced by pressure gradients in panels a, b and c, respectively.







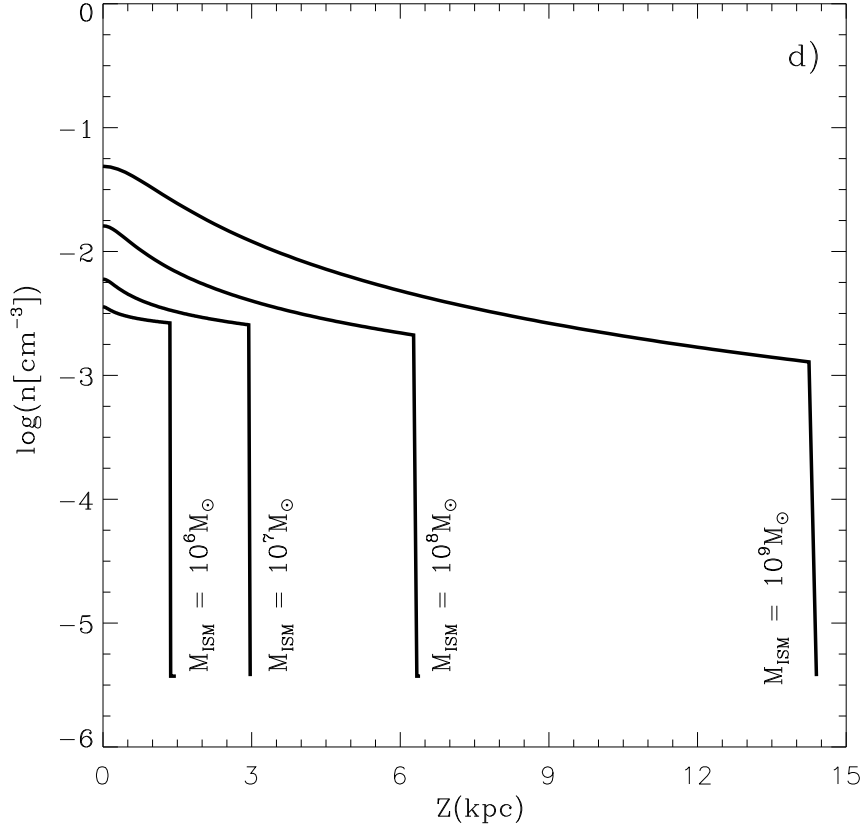


Fig. 2.— The density distribution. Solid lines in Panels a and b show the density distribution along the symmetry axis, derived for disk-like galaxies (see Table 1) with $\epsilon = 0.9$ and a mass $M_{ISM} = 10^6 M_{\odot} - 10^9 M_{\odot}$, and intergalactic pressures equal to 1 and $100 \text{ cm}^{-3} \text{ K}$, respectively. The dashed lines represent the corresponding fit to the density distributions. Panels c and d show the corresponding density distributions that resulted for galaxies without rotation ($\epsilon = 0$).

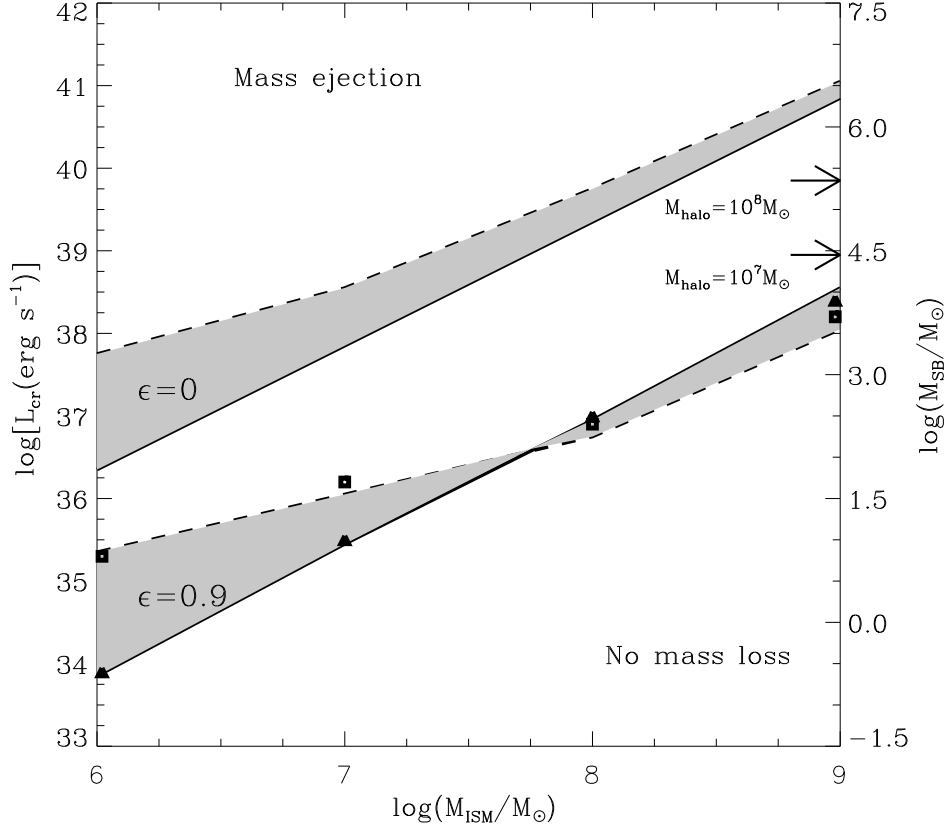


Fig. 3.— Energy estimates. The log of the critical mechanical luminosity, and of the starburst mass, required to eject matter from galaxies with a M_{ISM} in the range $10^6 - 10^9 M_{\odot}$. The lower limit estimates are shown for galaxies with extreme values of ϵ ($= 0$ and 0.9) and for two values of the intergalactic pressure $P_{\text{IGM}}/k = 1 \text{ cm}^{-3} \text{ K}$ (solid lines) and $P_{\text{IGM}}/k = 100 \text{ cm}^{-3} \text{ K}$ (dashed lines). The resolution of our numerical search is $\Delta \log L_{\text{cr}} = 0.1$. Each line should be considered separately as they divide the parameter space into two distinct regions: a region of no mass loss that is found below the line and a region in which blowout and mass ejection occur that is found above the line. Also indicated on the right-hand axis are the energy input rates required for a remnant to reach the outer boundary of a halo with mass $10^8 M_{\odot}$ and one with mass $10^7 M_{\odot}$, for the case of a gravitational potential provided by $M_{\text{DM}} = 9.1 \times 10^9 M_{\odot}$ that can hold an $M_{\text{ISM}} = 10^9 M_{\odot}$. The filled squares and triangles represent the analytical energy input rate estimated by means of equation (17), using the H_g values derived for the central Gaussian part of the disk-like density distributions shown in Figure 2 a, b.

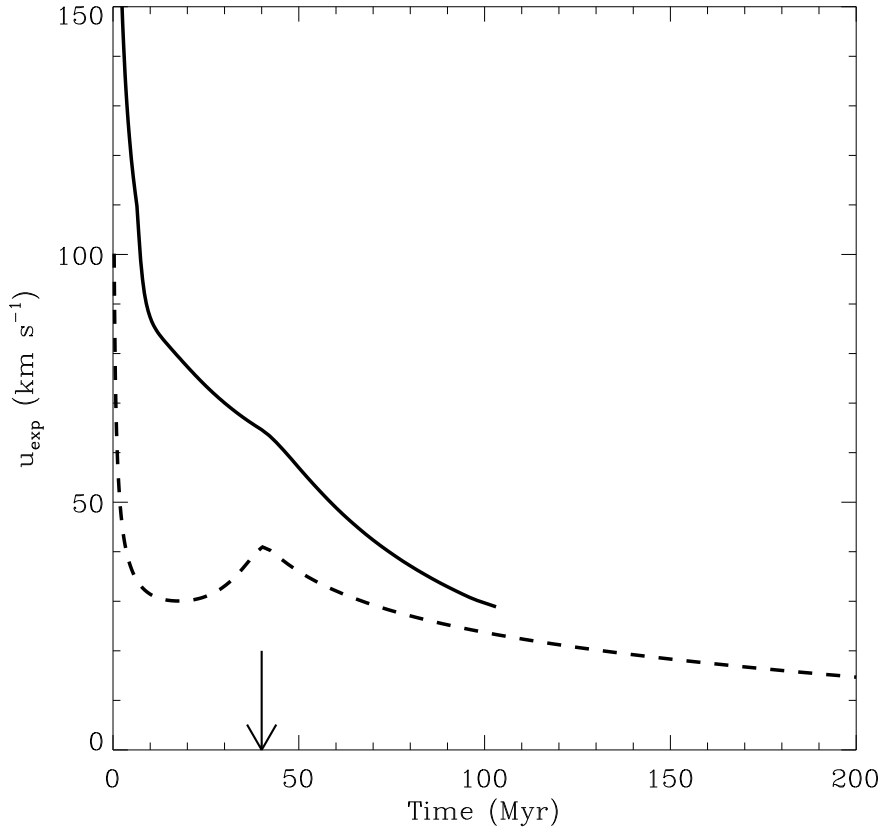


Fig. 4.— The maximum expansion speed measured along the symmetry axis Z for $10^8 M_{\odot}$ galaxy with spherical ISM density distribution. The solid line indicates the expansion velocity for $P_{\text{IGM}}/k=100$, whereas the dotted line represents the shell expansion for the $P_{\text{IGM}}/k=1$ model. The arrow indicates the end of the SB supernova phase. Note that the remnants require a much longer time to reach the outskirts of their host galaxy.

Table 1: Galaxy parameters.

Model	M_{DM} M_{\odot}	M_{ISM} M_{\odot}	R_{ISM} kpc	P_{IGM} nT/k	ϵ	C_{ISM} km s^{-1}	V_{esc} km s^{-1}	n_0 cm^{-3}	Z_{ISM} pc
M600.1	6.8×10^7	10^6	1.4	1.0	0.0	5.8	13.6	0.5	1400
M605.1	6.8×10^7	10^6	1.4	1.0	0.5	5.0	13.6	0.6	735
M609.1	6.8×10^7	10^6	1.4	1.0	0.9	2.8	13.6	0.7	135
M600.100	6.8×10^7	10^6	1.4	100	0.0	27.1	13.6	3.6×10^{-3}	1400
M605.100	6.8×10^7	10^6	1.4	100	0.5	22.7	13.6	5.2×10^{-3}	735
M609.100	6.8×10^7	10^6	1.4	100	0.9	15.5	13.6	9.6×10^{-2}	120
M700.1	3.5×10^8	10^7	3.0	1.0	0.0	8.8	22.5	1.2	3000
M705.1	3.5×10^8	10^7	3.0	1.0	0.5	7.7	22.5	1.4	1610
M709.1	3.5×10^8	10^7	3.0	1.0	0.9	4.1	22.5	2.1	279
M700.100	3.5×10^8	10^7	3.0	100	0.0	27.6	22.5	6.0×10^{-3}	3000
M705.100	3.5×10^8	10^7	3.0	100	0.5	25.4	22.5	6.5×10^{-3}	1645
M709.100	3.5×10^8	10^7	3.0	100	0.9	15.4	22.5	1.4×10^{-2}	279
M800.1	1.8×10^9	10^8	6.5	1.0	0.0	13.9	36.9	2.1	6500
M805.1	1.8×10^9	10^8	6.5	1.0	0.5	12.1	36.9	2.5	3520
M809.1	1.8×10^9	10^8	6.5	1.0	0.9	6.5	36.9	3.9	690
M800.100	1.8×10^9	10^8	6.5	100	0.0	30.4	36.9	1.6×10^{-2}	6500
M805.100	1.8×10^9	10^8	6.5	100	0.5	26.4	36.9	2.2×10^{-2}	3600
M809.100	1.8×10^9	10^8	6.5	100	0.9	15.2	36.9	4.2×10^{-2}	621
M900.1	9.1×10^9	10^9	14.2	1.0	0.0	22.3	60.4	3.0	14200
M905.1	9.1×10^9	10^9	14.2	1.0	0.5	19.5	60.4	3.7	7950
M909.1	9.1×10^9	10^9	14.2	1.0	0.9	11.0	60.4	4.3	1650
M900.100	9.1×10^9	10^9	14.2	100	0.0	39.2	60.4	4.9×10^{-2}	14200
M905.100	9.1×10^9	10^9	14.2	100	0.5	31.5	60.4	1.4×10^{-1}	7800
M909.100	9.1×10^9	10^9	14.2	100	0.9	19.0	60.4	1.8×10^{-1}	1650